GEOPHYSICAL RESEARCH LETTERS, VOL. 28, NO. 6, PAGES 1131-1134, MARCH 15, 2001

A test of magnetospheric radio tomographic imaging with IMAGE and WIND

S. A. Cummer,[1] M. J. Reiner,[2] B. W. Reinisch,[3] M. L. Kaiser,[4] J. L. Green,[5]
R. F. Benson,[4] R. Manning,[6] K. Goetz [7]

Abstract. Theoretical studies have shown the potential scientific value of multi-spacecraft radio tomographic imaging of the magnetosphere. The <10 R_E WIND perigee passes during August 2000 afforded a unique opportunity to test and verify the capabilities of radio tomography by measuring interspacecraft electromagnetic wave propagation parameters using the Radio Plasma Imager (RPI) on IMAGE as the transmitter and the WAVES instrument on WIND as the receiver. The primary goal of this experiment was to measure Faraday rotation variations in the RPI signal and interpret them in terms of the path-integrated magnetic field and electron density. A special 6 W linearly-polarized 828 kHz RPI signal was clearly detected by WAVES more than 6 R_E away and showed a distinct signature of time-varying Faraday rotation. We show how changes in the path-integrated electron density/magnetic field product can be unambiguously measured from this continuous, low signal to noise ratio, single frequency measurement.

1. Introduction

Radio tomography is commonly used for large scale remote sensing of the ionosphere [*Bernhardt et al.*, 1998] and has been proposed in two distinct forms for magnetospheric remote sensing [*Ergun et al.*, 2000; *Ganguly et al.*, 2000]. The technique uses multiple receivers and transmitters to measure a path-integrated quantity on line-of-sight propagation paths. The information from these multiple paths is then assembled into an image of the probed quantity. *Ergun et al.* [2000] have studied the concept of a 16 spacecraft magnetospheric tomography mission based on interspacecraft phase difference and group delay measurements. These quantities are proportional to the path-integrated electron density, images of which can be tomographically generated from multiple satellite-to-satellite magnetospheric propagation paths. The concept of electron density remote sensing with this technique was proven with a two spacecraft experiment with ISEE 1 and 2 [*Harvey et al.*, 1978; *Hubert et al.*, 1998].

Ganguly et al. [2000] have shown how interspacecraft Faraday rotation measurements enable tomographic imaging of different magnetospheric parameters. Faraday rotation is the rotation of the polarization of a linearly polarized wave as it travels through an anisotropic medium, like magnetospheric plasma. For frequencies higher than the electron plasma and gyrofrequencies, the Faraday rotation angle θ_F is proportional to the path-integrated product of the electron density N_e and the magnetic field $\mathbf{B}$ parallel to the wave vector k, or

$$\theta_F = K \int_p N_e \frac{\mathbf{k}}{|\mathbf{k}|} \cdot \mathbf{B}\, dl, \tag{1}$$

where $K = q^3(2\epsilon_0 c m_e^2 \omega^2)^{-1}$ [*Budden*, 1985, p. 374]. Thus, a single path Faraday rotation measurement contains information about the electron density and magnetic field along that path, and multiple paths through the same volume of space can be assimilated into a tomographic image of this combined quantity through a number of different reconstruction methods [*Raymund*, 1995]. *James and Calvert* [1998] reported a related rocket experiment in which the magnetic field and electron density along the path between a dual payload transmitter-receiver pair were inferred from measurements of Faraday rotation. However, Faraday rotation measurements on satellite-to-satellite propagation paths have yet to be reported.

Combined Faraday rotation and phase difference measurements have been used to separate the ionospheric and plasmaspheric contributions to the total column-integrated electron content in spacecraft-ground propagation experiments [*Garriott et al.*, 1970]. A combination of these two techniques can also independently measure electron density and magnetic field in the magnetosphere [*Ganguly et al.*, 2000] and would enable novel and valuable large-scale measurements.

Two existing flight instruments afforded a unique opportunity to test the concept of magnetospheric radio remote sensing and imaging with Faraday rotation. The Radio Plasma Imager (RPI) [*Reinisch et al.*, 2000] on the Imager for Magnetopause-to-Aurora Global Exploration (IMAGE) satellite [*Burch*, 2000] is an active sounder that operated as the transmitter in this experiment, and the WAVES receiver [*Bougeret et al.*, 1995] on the WIND satellite operated as the receiver. During two separate passes, the RPI signal was clearly received by WAVES. The signal showed time-varying Faraday rotation which we interpret in terms of spatially-varying magnetospheric medium between the two spacecraft.

[1]Electrical and Computer Engineering Department, Duke University, Durham, North Carolina
[2]RITSS/LEP, NASA Goddard Space Flight Center, Greenbelt, Maryland
[3]Center for Atmospheric Research, University of Massachusetts-Lowell, Lowell, Massachusetts
[4]Laboratory for Extraterrestrial Physics, NASA Goddard Space Flight Center, Greenbelt, Maryland
[5]Space Science Data Operations Office, NASA Goddard Space Flight Center, Greenbelt, Maryland
[6]Observatoire de Paris, Meudon, France
[7]School of Physics and Astronomy, University of Minnesota, Minneapolis, Minnesota

Paper number 2000GL012683.
0094-8276/01/2000GL012683$05.00

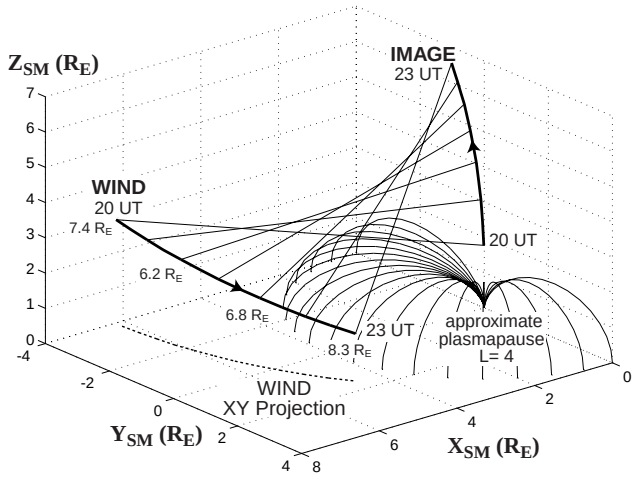

Figure 1. WIND and IMAGE trajectories from 2000–2300 UT on August 15, 2000. Also shown are the propagation paths between the spacecraft, each labeled with the interspacecraft distance, and an approximate plasmapause location.

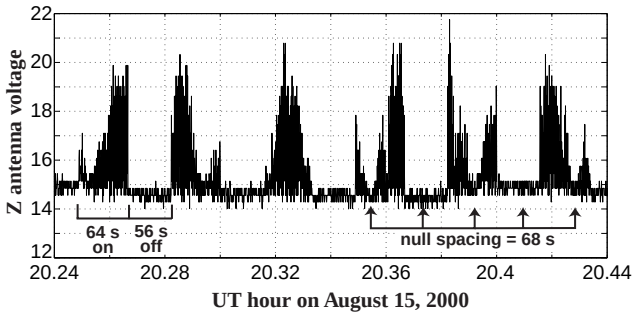

Figure 3. Close-up of RPI signal. The spin-induced sinusoidal signal modulation shows clear nulls that correspond to a 136 s spin period, while the actual IMAGE spin period is 122.7 s. The difference is created by time-varying Faraday rotation on the propagation path.

2. The Experiment

A series of WIND petal orbits brought the spacecraft within 4 R_E of Earth during August 2000. More importantly, WIND passed within 6 R_E of IMAGE during these periods. On August 3–4, 2000 between 2250 and 0050 UT, and on August 15–16, 2000 between 1950 and 0000 UT, RPI transmitted a 6 W linearly polarized signal on one of its spinning dipole antennas. An 828 kHz single frequency transmission repeated a 2 minute cycle of 64 seconds of 0.5 seconds on/0.5 seconds off modulation, followed by 56 seconds of silence. The frequency was chosen to maximize the transmitted power and to be significantly higher than auroral kilometric radiation (AKR) frequencies to maximize the signal to noise ratio (SNR) at WIND. WAVES received the RPI signal on both days, but the sampling rate was much faster (every 358 ms on spin axis-aligned Z antenna) on August 15, and we focus on these data in this paper. We emphasize that the data analyzed in this paper were received by a non-spinning dipole. Figure 1 shows the IMAGE and WIND trajectories from 2000–2300 UT on August 15 with the propagation paths between the spacecraft. Also drawn is the $L = 4$ surface, which is a rough estimate of the plasmapause location. Between these times, the propagation paths are likely outside the plasmapause.

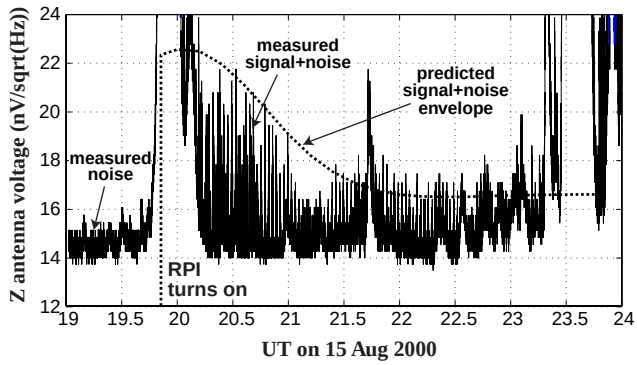

Figure 2. The measured Z antenna signal at 828 kHz during the experiment. The noise floor is predominantly galactic background radiation, and the clear spikes from 20–23 UT are the RPI signal. The dotted line shows the predicted signal envelope, assuming 6 W transmitted. It agrees well with the envelope of the measured RPI signal.

Figure 2 shows the Z antenna voltage at 828 kHz in a 3 kHz bandwidth received by WAVES during this period. The noise floor is mostly galactic background [*Novaco and Brown*, 1978], which fundamentally limits the distance over which the RPI signal can be received. Solar radio emissions (20 UT) and AKR-induced receiver intermodulation distortion (23.5 UT) occasionally dominate the received signal, but during most periods the RPI signal, with a distinct 64 s on, 56 s off modulation, is clearly visible. Faster amplitude variations during the 64 s on periods (not distinct in Figure 2) are from the varying overlap of the 0.5 s on, 0.5 s off modulation and the signal integration time, which is slightly less than the 358 ms sampling period.

Assuming 6 W of transmitted power (M. Haines, personal communication) and accounting for the directional antenna gain, the propagation loss, and antenna capacitance loss [*Manning and Fainberg*, 1980], we can calculate the theoretical total received voltage envelope $S_{\rm tot}(t) = \sqrt{P_{\rm sig}(t) + P_{\rm noise}}$, where $P_{\rm sig}(t)$ is the received signal power, and $P_{\rm noise}$ is the constant background noise power. The WAVES detector is an RMS detector, so the noise and signal powers add linearly. This predicted signal envelope $S_{\rm tot}$ is plotted on Figure 2. The agreement between the predicted and measured envelopes is, on average, better than 10%, indicating that the propagation of this signal is close to what it would be in free space. This result is expected because the 828 kHz signal frequency is significantly higher than the expected electron gyro- and plasma frequencies on these propagation paths. Even though the SNR is low (less than unity for part of this period), the received RPI signal is distinct.

3. Measuring Faraday Rotation

The IMAGE spacecraft and the RPI transmitting dipole spun clockwise (from WIND's perspective) with a 122.7 s spin period. This spin generates a sinusoidal signal amplitude modulation that is visible in the data. A close examination of the signal nulls, however, shows that they do not occur precisely every half spin period. The 64 second

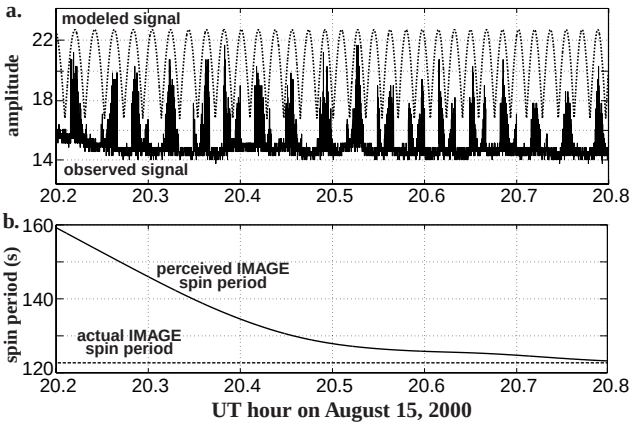

Figure 4. a: Modeled and measured RPI signal. The modeled signal is designed to match the time-varying spin modulation of the measured signal. b: The perceived spin period used to generate the modeled signal.

duration of the signal "on" period usually spans an entire half spin period and therefore unambiguously shows times of signal minima and maxima. Figure 3 shows a close-up of a section of the data where these nulls occur 68 s apart, implying a perceived source spin period of 136 s. This spin period discrepancy varies with time and is due to the time-varying Faraday rotation of the electric field of the received signal. The polarization of a signal with time-varying Faraday rotation will rotate even if the source polarization is fixed, thus making the source look as though it were spinning. Similarly, a spinning source will appear to have its spin period altered by time-varying Faraday rotation. The sum of the received polarization angle is the sum of the transmitted polarization angle and the total Faraday rotation, and after differentiating in time, we find that

$$f_{\rm per}(t) = f_{\rm src}(t) + \frac{1}{2\pi}\frac{d\theta_F}{dt}, \qquad (2)$$

where $f_{\rm per}(t)$ and $f_{\rm src}(t)$ are the perceived and actual source spin frequencies, respectively, and $\theta_F(t)$ is the total Faraday rotation along the propagation path in radians. We define the Faraday rotation θ_F as positive in a right-hand sense with respect to the vector from transmitter to receiver, and the $f(t)$ terms are positive for rotation in the same right hand direction.

Thus by measuring $f_{\rm per}(t)$ from the data, we can find $d\theta_F/dt$ and thereby measure variations in the intervening magnetospheric medium. We iteratively find a smooth $f_{\rm per}(t)$ that makes the nulls of a modeled signal $S_{\rm mod}(t) \propto \cos(2\pi f_{\rm per}(t)t + \phi)$ match the times of the measured signal nulls. Figure 4a shows that the spin modulation of the measured signal and the modeled signal $S_{\rm mod}(t)$ match well. The following analysis is relatively insensitive to small perturbations in this fit.

Figure 4b shows the perceived spin period $1/f_{\rm per}(t)$. The perceived spin frequency is smaller than the actual spin frequency and is increasing. Both of these frequencies are negative, however, by our right hand sign convention, thus (2) indicates that $d\theta_F/dt$ is positive and approaching zero during the 20.2–20.8 UT period. We focus in this paper on the analysis of the data from 20.2–21.2 UT because after 2112 UT, the lower SNR obscures the spin modulation. We emphasize, however, that the spin modulation is distinct during the studied period, when further analysis shows that the SNR is between only 0.9 and 1.2.

4. Magnetospheric Radio Remote Sensing

The goal of radio tomographic remote sensing is to measure a path-integrated quantity over multiple propagation paths. From (1), we can write the path-integrated quantity in terms of our measured $d\theta_F/dt$ as

$$Q(t) = \int_p N_e \frac{\mathbf{k}}{|\mathbf{k}|}\cdot\mathbf{B}\,dl = \frac{1}{K}\left(\theta_F(0) + \int_0^t \frac{d\theta_F}{d\tau}\,d\tau\right). \qquad (3)$$

Except an undetermined initial constant $\theta_F(0)$, we can measure $Q(t)$ from the spin rate of the single frequency signal. The continuity of the spin rate measurement ensures a high precision, unambiguous polarization measurement from a single frequency, low SNR signal observed with a single antenna. Figure 5 shows the measured change in $Q(t)$ as a function of time. The data are consistent with a smooth increase in the path-integrated product of electron density and $\mathbf{k}$-directed magnetic field. Aside from the undetermined initial constant, this measured $Q(t)$ is what is needed to implement magnetospheric radio tomography. With more detailed analysis, we can determine whether the observed changes agree with those predicted by electron density and magnetic field models, and we can even attempt a true tomographic reconstruction of the data under certain simplifying assumptions. These results will be discussed in a later paper.

The above spin rate-based method has advantages compared to other methods for measuring Faraday rotation. It only requires one antenna, while measuring polarization directly usually requires two orthogonal antennas. The continuity of the measured spin rate in the single antenna method also ensures that 180° changes in Faraday rotation are unambiguously measured. With direct polarization measurements, the signal must be sampled fast enough to ensure that 180° changes are not missed. The spin rate method is also robust and accurate in low SNR situations. There is an inherent smoothing of the measured Faraday rotation over one spin period with this method, however, so small scale variations could be missed. With a better SNR and a continuous transmitted signal, smaller variations might also be detectable.

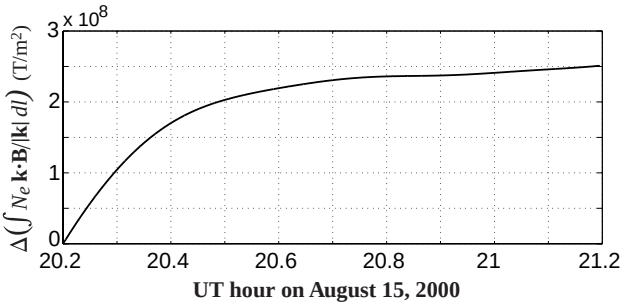

Figure 5. Change in the path-integrated electron density/magnetic field product measured from the observed Faraday rotation change.

What this method lacks is the ability to measure the absolute Faraday rotation. One way to obtain absolute measurements is to measure the Faraday rotation difference between two frequencies that are close enough that the rotation difference is less than 180°. The sensitivity of differential Faraday rotation to small magnetospheric changes is poor, however, because the entire path must generate less than 180° of differential rotation. The sensitivity of the spin-rate method to small changes in $Q(t)$ can be much higher because of the ability to detect multiple 180° changes. Combining the two techniques in a composite method, using differential Faraday rotation to provide absolute measurements and polarization spin rate to precisely measure small Faraday rotation changes, may enable more accurate and precise magnetospheric radio remote sensing.

5. Conclusions

A 6 W single frequency transmission from IMAGE/RPI was successfully observed by WIND/WAVES during two experiments designed to test the concept of magnetospheric radio tomographic imaging. The time-varying perceived spin rate of the signal is a clear signature of time-varying Faraday rotation on the propagation path. We measure changes in the path-integrated product of magnetic field and electron density directly from the observed Faraday rotation changes. This path-integrated quantity is the basis for measuring the product of magnetic field and electron density with magnetospheric radio tomography.

The implemented spin rate measurement is a straightforward way to sensitively measure Faraday rotation changes with a single-frequency transmission and a single receiving antenna without any 180° rotation ambiguities. This method combined with another to measure the absolute Faraday rotation at some point during the observing period, such as a dual frequency differential Faraday rotation measurement, can precisely measure the path-integrated product of magnetic field and electron density.

This experiment demonstrates the feasibility of a new and potentially valuable magnetospheric radio remote sensing technique. A combination of total Faraday rotation measurements, as described here, and phase difference measurements, as mentioned in the introduction, is a promising method to measure electron density and magnetic field over a large volume of space simultaneously with only a few spacecraft.

Acknowledgments. We thank the RPI and WAVES teams for their expert assistance in arranging and implementing the reported experiment. BWR was supported by NASA under subcontract 83822 from SwRI.

References

Bernhardt, P. A., et al., Two-dimensional mapping of the plasma density in the upper atmosphere with computerized ionospheric tomography (CIT), *Phys. Plasmas*, *5*, 2010–21, 1998.

Bougeret, J.-L., et al., WAVES: The radio and plasma wave investigation on the WIND spacecraft, *Space Sci. Rev.*, *71*, 231–263, 1995.

Budden, K. G., *The Propagation of Radio Waves*, Cambridge Univ. Press, New York, 1985.

Burch, J. L., IMAGE mission overview, *Space Sci. Rev.*, *91*, 1–14, 2000.

Ergun, R. E., et al., Feasibility of a multisatellite investigation of the Earth's magnetosphere with radio tomography, *J. Geophys. Res.*, *105*, 361–73, 2000.

Ganguly, S., G. H. Van Bavel, and A. Brown, Imaging electron density and magnetic field distributions in the magnetosphere: A new technique, *J. Geophys. Res.*, *in press*, 2000.

Garriott, O. K., A. V. Da Rosa, and W. J. Ross, Electron content obtained from Faraday rotation and phase path length variations, *J. Atmos. Terr. Phys.*, *32*, 705–727, 1970.

Harvey, C. C., J. Etcheto, Y. De Javel, R. Manning, and M. Petit, The ISEE electron density experiment, *IEEE Trans. Geosci. Electr.*, *GE-16*, 231–8, 1978.

Hubert, D., C. C. Harvey, M. Roth, and J. De Keyser, Electron density at the subsolar magnetopause for high magnetic shear: ISEE 1 and 2 observations, *J. Geophys. Res.*, *103*, 6685–92, 1998.

James, H. G., and W. Calvert, Interference fringes detected by OEDIPUS C, *Radio Sci.*, *33*, 617–29, 1998.

Manning, R., and J. Fainberg, A new method of measuring radio scource parameters of a partially polarized distributed source from spacecraft observations, *Space Sci. Inst.*, *5*, 161, 1980.

Novaco, J. C., and L. W. Brown, Nonthermal galactic emission below 10 megahertz, *Astrophys. J.*, *221*, 114, 1978.

Raymund, T. D., Comparisons of several ionopsheric tomography algorithms, *Ann. Geophys.*, *13*, 1254–62, 1995.

Reinisch, B. W., et al., The Radio Plasma Imager investigation of the IMAGE spacecraft, *Space Sci. Rev.*, *91*, 319–359, 2000.

R. F. Benson, M. L. Kaiser, M. J. Reiner, Laboratory for Extraterrestrial Physics, NASA GSFC, Greenbelt, MD, 20771.

S. A. Cummer, Electrical and Computer Engineering Department, Box 90291, Duke University, Durham, NC 27708. (cummer@ee.duke.edu)

K. Goetz, School of Physics and Astronomy, University of Minnesota, Minneapolis, MN 55455.

J. L. Green, Code 630, NASA GSFC, Greenbelt, MD 20771.

R. Manning, Observatoire de Paris, Meudon, France.

B. W. Reinisch, Center for Atmospheric Research, University of Massachusetts-Lowell, Lowell, MA 01854.

(Received November 22, 2000; accepted January 03, 2001.)